Preprints of the 23rd IFAC World Congress
Busan, Republic of Korea, August 23-28, 2026

Citation: Juan Garcia-Lechuz, Rosario Aragues, and Gonzalo Lopez-Nicolas. Distributed multi-target enclosing control framework for a split and merge task. 23rd IFAC World Congress Busan, Republic of Korea, August 23-28, pages 67-72, 2026

Distributed multi-target enclosing control framework for a split and merge task

Juan García-Lechuz * **Rosario Aragüés** *
Gonzalo López-Nicolás *

* *Instituto de Investigación en Ingeniería de Aragón (I3A), Universidad de Zaragoza, Mariano Esquillor, 50018 Zaragoza, Spain (e-mail: jgarcialechuz@unizar.es, raragues@unizar.es, gonlopez@unizar.es)*

Abstract: This paper studies the problem of cooperative multi-target enclosing. More specifically, we propose a distributed control framework to address the case where it is necessary to split or merge the team of agents as the distance between target groups increases or decreases, respectively. We first present a multi-target enclosing control law combining an affine formation control law with distance-based control terms to adjust formations around targets. Then, a novel weight matrix design is proposed for affine formation control of regular polygons. The distributed nature of this weight design method allows agents to locally compute the weights so that they can reorganize in subgroups or merge while ensuring convergence. Stability analysis of the proposed weight design method is included, as well as a numerical simulation using the proposed enclosing control to illustrate the splitting and merging task.

Keywords: Formation control, multi-agent systems, distributed control.

1. INTRODUCTION

In target-enclosing systems, multiple agents cooperate to surround and track one or more targets. Early approaches established distributed conditions for surrounding the target, ensuring stability and convergence through rules based on angles and distances. In particular, Hara et al. (2008) used cyclic pursuit strategies to induce stable orbital trajectories around a moving target, without a global reference or centralized communication. To address the enclosing of multiple targets, Zhang et al. (2015) presented a distributed method that preserves circular patterns and topological relationships among agents. More recently, Aranda et al. (2021) used the adaptation of the rotation and scale of the formation to improve target tracking and agents' distribution. On the other hand, Liu et al. (2023) proved that, using relative measurements, the geometric center of the formation converges to the target while preserving the desired formation. All these methodologies used multi-agent formation control to organize the team around the targets. However, this formation is unique and cannot be adapted if the targets are split into separate clusters.

Maintaining specific geometric formations while maneuvering is crucial for a wide range of applications, including target enclosing scenarios (López-Nicolás et al. (2020)). In particular, distributed formation control strategies design control laws to maintain relative configurations between agents, without the need for global data. Many approaches, such as the one presented by Falconi et al. (2011), are based on graph properties and Laplacian matrices. One of these strategies was proposed in Wang et al. (2012, 2013) to control a team of single integrator agents towards a desired 2D formation up to scale, using a complex Laplacian-like weight matrix. A systematic construction method of the complex Laplacian matrix was later proposed by Lin et al. (2014, 2015), who also studied the necessary graphical conditions to ensure convergence. Laplacian matrix-based control was extended to 3D formations in Lin et al. (2016). They studied the affine formation control, using a matrix with both positive and negative weights, and established the necessary graphical conditions for stability. In another contribution, Zhao et al. (2018) included motion constraints in the affine formation control of selected agents, converging to a unique solution tailored to the environment. Regarding convergence to constrained formations, Fathian et al. (2017) proposed a control based on relative positions, including a distance-based control term to control the scale of the formation.

The present paper addresses the problem of cooperative multi-target enclosing. A distributed control method is proposed using a novel weight design for affine formation control of regular polygons. This weight design allows agents to locally compute the control law to converge to an affine transformation of a regular polygon. Lastly, to enclose multiple targets, additional distance-based control terms are proposed to adjust formations around targets. This paper seeks to extend traditional methods, considering single targets and multi-target scenarios, to the case in which it is necessary to split the team of agents when the distance between target groups increases, or merge the team if the targets come back together.

⋆ This work was supported via project REMAIN - S1/1.1/E0111 (Interreg Sudoe Programme, ERDF), via projects PID2021-124137OB-I00 and PID2024-159279OB-I00 funded by MICIU/AEI/10.13039/501100011033, by ERDF/EU, and via grant PRE2022-10422

©2026 the authors. Accepted by IFAC for publication under a Creative Commons Licence CC-BY-NC-ND

2. PROBLEM STATEMENT

We consider a team of $n \in \mathbb{N}$ agents in $\mathbb{R}^2$, with $n \geq 5$. During the control, this team of agents splits into groups of d agents, with $5 \leq d \leq n$, and the inter-agent sensing topology of a group is always described by a squared cycle graph $\mathcal{G}_d = (\mathcal{V}_d, \mathcal{E}_d)$, where $\mathcal{V}_d = \mathbb{N}_d = \{1, 2, ..., d\}$ is the set of vertices, and $\mathcal{E}_d \subset \mathcal{V}_d \times \mathcal{V}_d$ is the set of edges. Each vertex of the graph represents an agent.

Definition 1. Given a squared cycle graph of d agents $\mathcal{G}_d = (\mathcal{V}_d, \mathcal{E}_d)$, with $d \geq 5$, the set of neighbors of agent $i \in \mathcal{V}_d$ is denoted by:

$$\mathcal{N}_i = \{(i-2),\, (i-1),\, (i+1),\, (i+2)\}. \tag{1}$$

In (1) and from now on, we refer to the agents indices as *cyclic*, meaning that if $i = d$, then $i+1 = 1$ and $i+2 = 2$, and if $i = 1$, then $i-1 = d$ and $i-2 = d-1$, and similarly with $i = 2$, and $i = d-1$.

If $i \in \mathcal{V}_d$ and $j \in \mathcal{V}_d$ are neighbors, i can measure the relative position of j in its local coordinate frame, denoted as ${}^i q_j = R_i^{-1}(q_j - q_i)$, being $R_i \in SO(2)$ the rotation matrix of the local coordinate frame of agent i with respect to the global coordinate frame. The state of the agents in global coordinates is defined by the column vector $q = [q_1^\top, q_2^\top, ..., q_d^\top]^\top \in \mathbb{R}^{2d}$, being $q_i \in \mathbb{R}^2$ the state of agent i. Single integrator dynamics govern each agent:

$${}^i\dot{q}_i = {}^i u_i, \tag{2}$$

where ${}^i u_i \in \mathbb{R}^2$ represents the control input of agent i in its local coordinate frame. We want the team of agents to enclose a set of m targets whose positions in global coordinates are defined by $c = [c_1^\top, c_2^\top, ..., c_m^\top]^\top \in \mathbb{R}^{2m}$, and can be distanced to the point of splitting targets into subgroups. We assume that all agents can measure the relative position of the centroid of the target subgroups.

Definition 2. Let us consider the *d-enclosing* formation:

$$\mathcal{Q}_d = [q_1^{*\top}, q_2^{*\top}, ..., q_d^{*\top}]^\top \in \mathbb{R}^{2d}, \tag{3}$$

in global coordinates, being $q_i^* \in \mathbb{R}^2$ the state of agent i in the formation. This formation is a centered regular polygon with d vertices, which is defined as:

$$q_k^* = r\,[cos\theta_k, sin\theta_k]^\top, \qquad \theta_k = \theta\,(k-1), \qquad k = 1, ..., d. \tag{4}$$

with r and $\theta = \frac{2\pi}{d}$ the radius and the central angle of the regular polygon, respectively. Thus, $\mathcal{Q}_d$ is equivalent to a circle formation, as it guarantees both equidistant spacing and uniform radial distance from a common center. Given the following rotation matrix in $SO(2)$:

$$R_\theta = \begin{bmatrix} cos\theta & -sin\theta \\ sin\theta & cos\theta \end{bmatrix}, \tag{5}$$

the *d-enclosing* formation fulfills that $q_k^* = R_\theta\, q_{k-1}^*$, with $k = 2, ..., d$, and $q_1^* = R_\theta\, q_d^*$.

The problem to be solved is as follows: Consider a team of n agents in $\mathbb{R}^2$ and a set of m targets that may split into multiple spatial clusters. It is assumed that each agent: (i) knows when to split and merge given the distance between target clusters, (ii) knows which target cluster to enclose, and (iii) knows the number of agents d that enclose its corresponding cluster. This information can be provided by a higher-level decision module or negotiated among agents. The focus of this work is the design of the low-level distributed control law that, given this information, drives the agents to form and maintain the enclosing formations. In addition, it is assumed that, for each cluster, the d agents that will perform the enclosing communicate according to the graph $\mathcal{G}_d$ as in Definition 1. The maintenance of this communication topology is handled externally and is outside the scope of this work. Thus, the problem is to design a distributed control law such that:

- The agents organize into one or several *d-enclosing* formations that enclose their assigned clusters.
- Knowing d and $\mathcal{N}_i$, each agent computes its own control law, based on relative position measurements, so that the team can split into multiple sub-formations when the targets separate, or merge sub-formations when target clusters come sufficiently close.

3. AFFINE FORMATION CONTROL OF *d-ENCLOSING* FORMATIONS

3.1 Preliminaries

The set of affine transformations of a *d-enclosing* formation $\mathcal{Q}_d$ can be written as

$$\mathcal{A}(\mathcal{Q}_d) = \{(I_d \otimes B)\mathcal{Q}_d + 1_d \otimes b \mid B \in \mathbb{R}^{2\times 2}, b \in \mathbb{R}^2\}, \tag{6}$$

where b represents a translation and B is any linear transformation matrix.

Definition 3. The set $\mathcal{A}(\mathcal{Q}_d)$ in (6) is henceforth referred to as the *d-affset*.

If the state q belongs to the *d-affset*, the d agents form an affine transformation of a *d-enclosing* formation.

Let us define the following augmented formation matrix $D = [D_1^\top, ..., D_d^\top]^\top \in \mathbb{R}^{d\times 3}$ for the *d-enclosing* formation of unitary radius, such that:

$$D_k = [1, q_k^*], \qquad \forall k = 1, ..., d, \tag{7}$$

According to the result for a generic augmented formation matrix in Lemma 4 of Zhao (2018), the subspace of the *d-affset* (6) can also be written using D as:

$$\mathcal{A}(\mathcal{Q}_d) = \mathrm{Col}(D \otimes I_2), \tag{8}$$

with Col(.) the column space of a matrix and $I_2 \in R^{2\times 2}$ the identity matrix.

Definition 4. The orthogonal projection matrix $P \in \mathbb{R}^{2d\times 2d}$ that projects any vector $v \in \mathbb{R}^{2d}$ onto the space spanned by the columns of $D \otimes I_2$, i.e, onto $\mathcal{A}(\mathcal{Q}_d)$ so that

$$v' = P\,v, \quad v' = P\,v' \quad \text{with } v' \in \mathcal{A}(\mathcal{Q}_d), \tag{9}$$

can be written as:

$$P = (D \otimes I_2)((D \otimes I_2)^\top (D \otimes I_2))^{-1}(D \otimes I_2)^\top. \tag{10}$$

Equivalently, by the properties of the Kronecker product:

$$P = \mathcal{P} \otimes I_2, \quad \text{with } \mathcal{P} = D(D^\top D)^{-1}D^\top \in \mathbb{R}^{d\times d}. \tag{11}$$

As stated in Definition 0.9.13, Chapter 0 of Horn and Johnson (2012), this matrix is symmetric and idempotent.

3.2 Control law

To address multi-agent formation control, we build up from the following strategy (Lin et al. (2014)):

$${}^i u_i = \sum_{j\in\mathcal{N}_i} A_{ij}\, {}^i q_j, \tag{12}$$

where $A_{ij} \in \mathbb{R}^{2\times 2}$ are constant control weight matrices designed and provided to agents in advance. If the matrices

A_{ij} and R_i commute, i.e., if $R_i A_{ij} = A_{ij} R_i$, then the closed-loop dynamics of the agents in global coordinates can be expressed as:

$$\dot{q} = Aq, \tag{13}$$

in which $A = [A_{ij}] \in \mathbb{R}^{2d \times 2d}$, with $A_{ii} = -\sum_{j \in \mathcal{N}_i} A_{ij}$, and $A_{ij} = 0_{2\times 2}$ (the all-zeros matrix of size 2×2) for $j \notin \mathcal{N}_i$ (i.e., when agents are not neighbors).

Definition 5. Let us define $A_{ij} = a_{ij} I_2 \ \forall A_{ij} \neq 0_{2\times 2}$, where a_{ij} is a scalar weight. Then, it is trivial to show that $A_{ij} R_i = R_i A_{ij}$. The matrix composed of the scalar weights a_{ij} is also defined as $\Omega = [a_{ij}] \in \mathbb{R}^{d\times d}$, from which we define the matrix A as:

$$A = \Omega \otimes I_2. \tag{14}$$

Given the control law (13), from Lemma 4 in Zhao (2018), the stable matrix A that allows convergence to the *d-affset* must nullify this same vector space, i.e.:

$$\mathcal{A}(\mathcal{Q}_d) = \text{Null}(A) = \text{Null}(\Omega \otimes I_2), \tag{15}$$

with Null(.) the null space of a matrix. This ensures that:

$$\dot{q} = A\, q = (\Omega \otimes I_2)\, q = 0, \quad \forall q \in \mathcal{A}(\mathcal{Q}_d). \tag{16}$$

On the other hand, as demonstrated in Lin et al. (2016), $\mathcal{G}_d$ must satisfy the universal rigidity condition, so that A is negative-semidefinite and satisfies that $\text{rank}(A) = 2\,(d-3)$ in $\mathbb{R}^2$. Under these conditions, control (13) allows the team of agents to converge stably to a formation within the *d-affset*. In this way, the specific formation q^∞ achieved at the end of the control (12) depends on the initial configuration of the agents $q(0)$, so that:

$$q^\infty = P\, q(0). \tag{17}$$

4. MULTI-TARGET ENCLOSING

Given a subset of d agents, the objective of the multi-target enclosing task is to converge to a specific *d-enclosing* formation whose radius allows it to encircle the subset of targets considered within it. As an example, let us consider the whole target set. The radius ρ of the *d-enclosing* formation $\mathcal{Q}_d$ as in Definition 2 can be computed as:

$$\rho = \max_{1\leq i\leq m} \|c_i - \mu\| + \eta \quad \forall i = 1, ..., m, \tag{18}$$

with μ the centroid of the targets and η a predefined offset. From this radius, we can compute the distance between neighboring agents, that is, the side and the second-order chord of the *d-enclosing* formation, such that:

$$\ell_{ij} = \begin{cases} 2\,\rho\, sin\left(\dfrac{\pi}{d}\right) & \text{if } j \in \{i-1, i+1\}, \\ 2\,\rho\, sin\left(\dfrac{2\,\pi}{d}\right) & \text{if } j \in \{i-2, i+2\}. \end{cases} \tag{19}$$

4.1 Enclosing control law

As demonstrated in Zhao (2018), the affine control of *d-enclosing* formations converges specifically to a *d-enclosing* formation by adding constraints on the distances between at least three agents. Then, the control law in relative coordinates that allows the enclosing of c is of the form:

$$\begin{aligned} {}^i u_i = k_a \sum_{j\in\mathcal{N}_i} A_{ij}\, {}^i q_j \\ + k \sum_{j\in\mathcal{N}_i} (\|{}^i q_j\|^2 - \ell_{ij}^2)\, {}^i q_j + k\,(\|{}^i q_\mu\|^2 - \rho^2)\, {}^i q_\mu, \end{aligned} \tag{20}$$

where ${}^i q_\mu$ is the relative position of the centroid μ with respect to agent i, and $k_a > 0$ and $k > 0$ are constant control gains. In this control law, the first summand corresponds to the affine formation control law, and the next two are distance-based terms to restrict the distances between agents and between agents and the centroid.

4.2 Distributed weights design

This section proposes a method so that the weights in Ω can be obtained locally by each agent. This feature provides an advantage over other methods for calculating Laplacian-based weight matrices, such as the approaches proposed in Fathian et al. (2017) or Lin et al. (2016), which are based on a centralized precomputation of weights using optimization. We begin by demonstrating some properties of matrix P (11) and the *d-affset* $\mathcal{A}(\mathcal{Q}_d)$ (6), which will be used next for the weight design method.

Lemma 1. (*Invariability under cyclic permutations*) Let us define the cyclic permutation matrix $C_d \in \mathbb{R}^{d\times d}$, such that for any vector of the form $v = [v_1^\top, v_2^\top, ..., v_d^\top]^\top \in \mathbb{R}^{2d}$, and considering i a *cyclic* index, the following holds:

$$\begin{aligned} \nu &= (C_d \otimes I_2)\, v, \\ \nu_i &= v_{i-1}, \quad \forall i = 1, ..., d. \end{aligned} \tag{21}$$

Then, $\nu = (C_d \otimes I_2)\, v \in \mathcal{A}(\mathcal{Q}_d)$ iff $v \in \mathcal{A}(\mathcal{Q}_d)$.

Proof. If we consider $v \in \mathcal{A}(\mathcal{Q}_d)$, based on the definitions in (4) and (6), and considering the cyclic index i, the following equation holds:

$$\begin{aligned} \nu_i = v_{i-1} &= B\, q_{i-1}^* + b = B\, R_\theta^\top\, q_i^* + b \\ &= B' q_i^* + b, \quad \forall i = 1, ..., d. \end{aligned} \tag{22}$$

Hence, the matrix $B' = B\, R_\theta^\top$ is a linear transformation matrix, and we conclude that $(C_d \otimes I_2)\, v \in \mathcal{A}(\mathcal{Q}_d)$. □

***Theorem** 1.* (*Design of the orthogonal projector P*) Let $P = \mathcal{P} \otimes I_2 \in \mathbb{R}^{2d\times 2d}$ as in Definition 4 be the orthogonal projection matrix onto the *d-affset* $\mathcal{A}(\mathcal{Q}_d)$ (6). Then, $\mathcal{P} = \text{circ}(p)$ is a symmetric circulant matrix, and there is an expression for the elements of the first row $p_k \in \mathbb{R}^d$ of matrix $\mathcal{P}$, given by:

$$p_k = \frac{1}{d}\left(1 + 2\, cos\left(\frac{2\pi(k-1)}{d}\right)\right), \quad k = 1, ..., d. \tag{23}$$

Furthermore, the following equation is true for the eigenvalues of $\mathcal{P}$:

$$\lambda_l(\mathcal{P}) = \begin{cases} 1 \text{ if } l = 1, 2, d \\ 0 \text{ if } l \neq 1, 2, d. \end{cases} \tag{24}$$

Proof. Let us consider any generic vector $v \in \mathbb{R}^{2d}$. Given the properties in (9), the following conclusion is drawn from the result presented in Lemma 1:

$$P((C_d \otimes I_2)(P\, v)) = (C_d \otimes I_2)(P\, v). \tag{25}$$

Then, starting from the decomposition $v = Pv + (I_{2d} - P)v$, induced by the projector P, and using (25), the following expression is also true:

$$\begin{aligned} &P\,(C_d \otimes I_2)\, v = P((C_d \otimes I_2)(Pv)) \\ &+ P((C_d \otimes I_2)((I_{2d} - P)v)) = (C_d \otimes I_2)\, Pv \quad \forall v \in \mathbb{R}^{2d} \end{aligned} \tag{26}$$

where the second term in the sum is the projection of a vector from a subspace that is orthogonal to another

onto this same subspace. From this equation, using the mixed product property of the Kronecker product, it can be deduced that:

$$\begin{aligned} P\,(C_d \otimes I_2)\,v &= (\mathcal{P} \otimes I_2)\,(C_d \otimes I_2)\,v = ((\mathcal{P}\,C_d) \otimes I_2)\,v, \\ (C_d \otimes I_2)\,Pv &= (C_d \otimes I_2)\,(\mathcal{P} \otimes I_2)\,v = ((C_d\,\mathcal{P}) \otimes I_2)\,v. \end{aligned} \tag{27}$$

Equation (27) proves that $\mathcal{P}$ and C_d commute and thus, from Def. 0.9.6 of Horn and Johnson (2012), given that C_d is a circulant matrix, $\mathcal{P}$ is also a circulant matrix.

On the other hand, let us recall Definition 4 and the definition of θ_k in (4). The matrix $(D^\top D)^{-1}$ in (11) is the inverse of a diagonal matrix:

$$(D^\top D)^{-1} = \left(\sum_{k=1}^{d} D_k^\top\, D_k\right)^{-1} = \text{diag}\left[\frac{1}{d}, \frac{2}{d}, \frac{2}{d}\right]. \tag{28}$$

Now, considering $\mathcal{P} = [\mathcal{P}_{ik}]$, $\forall i, k = 1, ..., d$, we can obtain an expression for each element $\mathcal{P}_{ik}$ as:

$$\begin{aligned} \mathcal{P}_{ik} &= D_i\,\text{diag}\left[\frac{1}{d}, \frac{2}{d}, \frac{2}{d}\right] D_k^\top \\ &= \frac{1}{d} + \frac{2}{d}\,(cos\theta_i cos\theta_k + sin\theta_i sin\theta_k) \\ &= \frac{1}{d}\,(1 + 2\,cos(\theta_i - \theta_k))\,, \qquad \forall i, k = 1, ..., d. \end{aligned} \tag{29}$$

Then it is true that the particular equation for elements of the first row of matrix $\mathcal{P}$ can be written as:

$$\begin{aligned} p_k = \mathcal{P}_{1k} &= \frac{1}{d}(1 + 2\,cos(\theta_1 - \theta_k)) \\ &= \frac{1}{d}\left(1 + 2\,cos\left(\frac{2\pi(k-1)}{d}\right)\right), \qquad \forall k = 1, ..., d. \end{aligned} \tag{30}$$

Finally, given that $\mathcal{P}$ is a circulant matrix, from equation 2.2.9, Chapter 2 of Horn and Johnson (2012), the eigenvalues of $\mathcal{P}$ can be obtained from its generator p as:

$$\lambda_l(\mathcal{P}) = \sum_{k=0}^{d-1} p_{k+1}\, w^{k(l-1)}, \qquad \forall l \in \{1, ..., d\}, \tag{31}$$

where $w = e^{\frac{2\pi\,\imath}{d}}$, and $\imath$ is the imaginary unit. From the particular result in (23), equation (31) can be developed as follows:

$$\begin{aligned} \lambda_l(\mathcal{P}) &= \frac{1}{d}\sum_{k=0}^{d-1} e^{\frac{2\pi\,k(l-1)\imath}{d}} + \frac{1}{d}\sum_{k=0}^{d-1}(e^{\frac{2\pi\,k\,l\,\imath}{d}} + e^{\frac{2\pi\,k(l-2)\imath}{d}}) \\ &= \frac{1}{d}(d\,\delta_{l1}) + \frac{1}{d}(d\,\delta_{l0} + d\,\delta_{l2}) \\ &= \delta_{l1} + \delta_{ld} + \delta_{l2}, \qquad \forall l \in \{1, ..., d\}, \end{aligned} \tag{32}$$

where $\delta_{ll'}$, $\forall l' = 1, ..., d$, is the Kronecker delta of indexes l and l'. Then, 24 holds. □

Next, using the properties of $\mathcal{P}$ described in Theorem 1, a design for the weights in matrix Ω is proposed, ensuring the stability of the control (12).

***Theorem** 2. (Weights design)*
Consider a team of d single integrator agents with closed-loop dynamics (13). If $\Omega = \text{circ}(a)$ is a circulant matrix with the elements of a such that:

$$\begin{aligned} &a_1 < 0, \\ &a_2 = a_d = \frac{-a_1(cos(\theta) + 1)}{2cos(\theta) + 1}, \\ &a_3 = a_{d-1} = \frac{a_1}{2(2cos(\theta) + 1)}, \\ &a_k = 0 \qquad \forall k \notin \{1, 2, 3, d-1, d\}, \end{aligned} \tag{33}$$

where θ is as in Definition 2. Then, under the distributed local control law (12), starting from any initial configuration, the agents converge asymptotically stably to an affine formation in the *d-affset* $\mathcal{A}(\mathcal{Q}_d)$ (6).

Proof. From (15) and (8), one can conclude that matrices P and A must satisfy that $P\,A = 0$ and, using the mixed product property of the Kronecker product, that $\mathcal{P}\,\Omega = 0$. Let us consider Ω a circulant matrix, so that Ω and $\mathcal{P}$ can be diagonalized using the d-by-d Fourier transform matrix F, and related by the following equation:

$$\mathcal{P}\,\Omega = F\,(E_{\mathcal{P}}\,E_\Omega)\,F^{-1} = 0, \tag{34}$$

where $E_{\mathcal{P}}$ and E_Ω are the diagonal matrices composed of the eigenvalues of $\mathcal{P}$ and Ω, respectively. Recalling (24), we conclude that:

$$\lambda_l(\Omega) \begin{cases} = 0 \text{ if } l = 1, 2, d \\ \neq 0 \text{ if } l \neq 1, 2, d. \end{cases} \tag{35}$$

From the previously used expression for the eigenvalues of a circulant matrix, the eigenvalues of Ω are:

$$\begin{aligned} \lambda_l(\Omega) &= \sum_{k=0}^{d-1} a_{k+1}\, w^{k(l-1)} \\ &= a_1 + a_2(e^{\theta\,(l-1)\,\imath} + e^{-\theta\,(l-1)\,\imath}) \\ &+ a_3(e^{2\,\theta\,(l-1)\,\imath} + e^{-2\,\theta\,(l-1)\,\imath}) \\ &= a_1 + 2a_2\,cos(\theta(l-1)) + 2a_3\,cos(2\theta(l-1)) \\ &= a_1 + 2a_2\,cos(\theta(l-1)) \\ &+ 4a_3\,cos^2(\theta(l-1)) - 2a_3, \quad \forall l \in \{1, ..., d\}. \end{aligned} \tag{36}$$

If we substitute the expressions for a_k, $\forall k = 2, ..., d$, proposed in (33), into the expression for $\lambda_l(\Omega)$ in (36), the following expression holds:

$$\begin{aligned} \lambda_l(\Omega) &= \frac{2a_1(1 - cos(\theta(l-1)))(cos(\theta) - cos(\theta(l-1)))}{2cos(\theta) + 1}, \\ &\forall l \in \{3, ..., d-1\}. \end{aligned} \tag{37}$$

It can be noted that $cos(\theta(l-1)) \leq cos(\theta)$, $\forall l \neq 1$, and thus, considering that (33) imposes $a_1 < 0$:

$$\lambda_l(\Omega) < 0, \qquad \forall l \in \{3, ..., d-1\}. \tag{38}$$

From (35) and (38) we conclude that Ω is negative-semidefinite, with $\text{rank}(\Omega) = d-3$, meaning, A is negative-semidefinite, with $\text{rank}(A) = 2(d-3)$, which, as proven by Lin et al. (2016) ensures that control (12) is asymptotically stable to an equilibrium in the *d-affset* $\mathcal{A}(\mathcal{Q}_d)$ (6). □

Based on Definition 5 and Theorem 2, each row $\Omega_i \in \mathbb{R}^d$, $\forall i = 1, ..., d$, of Ω can be computed as:

$$\Omega_i = C_d^{i-1}\,a \qquad \forall i = 1, ..., d. \tag{39}$$

Thus, with knowledge of the identifiers of agents and neighbors, and the number of agents d and using (33) and (39), each agent i locally computes the weights that relate it to its neighbors $\mathcal{N}_i$ (Definition 1), while ensuring convergence of control (12) to a formation in the *d-affset* $\mathcal{A}(\mathcal{Q}_d)$ as in (6). Note that this approach is scalable since A is computed locally.

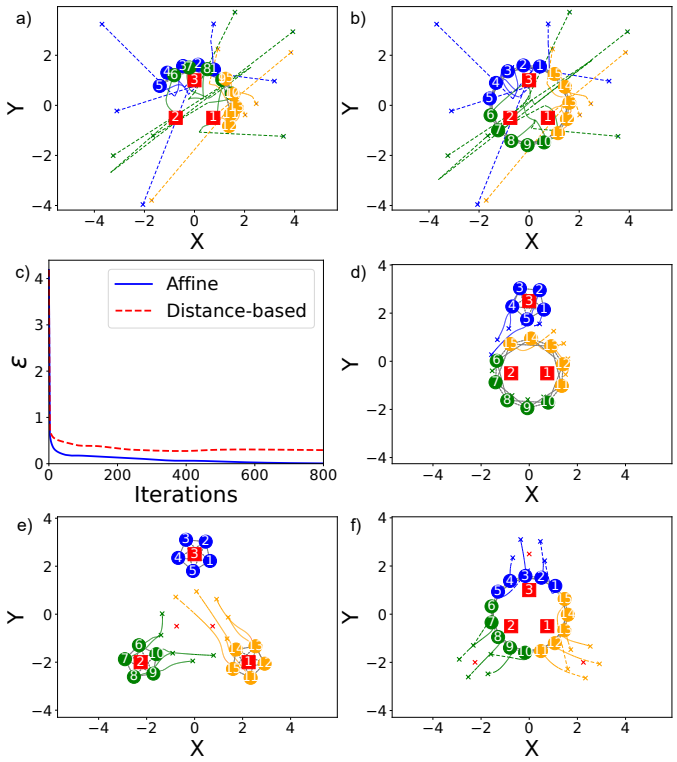

Fig. 1. Multi-target enclosing in a split and merge task. a) and b) Task 1 using only the distance-based control terms and control law (20), respectively. c) Comparison between ε using (20) and the distance-based control in Task 1. d) and e) Tasks 2 and 3, respectively: The agents split into groups to surround the targets. f) Task 4: The targets are back together, and the agents merge to enclose them.

4.3 Stability

***Theorem** 3. (Stability of the enclosing formation)* Consider the distributed local control law (20), with A computed as in Theorem 2. Then, if the following equation holds:

$$\frac{k_a}{k} > \frac{\gamma}{|\lambda_{\max}(A)|}, \tag{40}$$

with $\lambda_{\max}(A)$ the maximum non-zero eigenvalue of A, and

$$\gamma = 2 \max_i \sum_{j \in \mathcal{N}_i} \left| \|{}^i q_j(0)\|^2 - l_{ij}^2 \right| + \max_i \left(\|{}^i q_\mu(0)\|^2 + \rho^2 \right), \tag{41}$$

the multi-agent system converges asymptotically to the desired *d-enclosing* formation.

The proof of this theorem has been omitted due to space limits and follows from a Lyapunov analysis similar to the one in Th. 4.7 in Khalil and Grizzle (2002), and the fact that the distance-based terms in (20) are locally Lipschitz.

5. SIMULATIONS

To evaluate the performance of the method, a series of numerical simulations has been carried out in 2D. Furthermore, to study the convergence of control (20), the following inter-agent mean distance error is defined:

$$\varepsilon = \frac{1}{4\,d} \sum_{i=1}^{d} \sum_{j \in \mathcal{N}_i} \left(\|{}^i q_j\| - \|{}^i q_j^\infty\| \right) \tag{42}$$

being ${}^i q_j^\infty$ the relative state between agents in the formation q^∞ (17) obtained at the end of the control.

The following simulation consists of 15 agents ($n = 15$) governed by the control law (20). For the computation of ρ, an offset $\eta = 0.7$ has been chosen. In Fig. 1, agents are represented as numbered blue, green, and yellow dots. They will enclose three targets represented by red numbered squares in four consecutive tasks. In each task, the initial positions of agents are represented by crosses in their respective colors.

Task 1: Single-cluster encirclement. In Figs. 1a and 1b, the team of agents must enclose the three targets, starting from random positions. Figure 1a shows the case in which the control is based solely on distances. In this case, the control converges to a formation that respects distance constraints, but the agents are not evenly distributed around the targets. In Fig. 1b, law (20), with $k_a = 20, k = 2$, ensures affine formation control dominance, converging to $\mathcal{Q}_{15}$ while maintaining ρ around the targets' centroid. Figure 1c compares the inter-agent mean distance error ε in both cases and shows that the first case never reaches a formation in the 15-*affset*.

Task 2: Encirclement of two clusters. In Fig. 1d, targets are split into two clusters, while the agents recalculate their weights locally using (33), (39), and the knowledge of d and $\mathcal{N}_i$. The blue agents converge to a 5-*enclosing* formation around target 3, while the remaining agents form a 10-*enclosing* formation around targets 1 and 2.

Task 3: Encirclement of three clusters. In Fig. 1e, targets 1 and 2 are separated, and as a consequence, agents 6 to 15 split. In tasks 2 and 3, the affine formation control has to push the agents to surround the centroid, since otherwise they could gather in the section of the circumference closest to them to comply with the radius restriction.

Task 4: Merging. In Fig. 1f, the targets return to their initial position, and the agents merge in $\mathcal{Q}_{15}$ around them.

The left side of Fig 2 shows the distance error ε throughout the simulation of all the tasks. At the beginning of tasks 2 and 3 (iterations 800 and 2000), the distance error due to the change in connectivity is much lower than the error at the beginning of the simulation. This error is reduced in a very short time. Convergence speed in the affine term depends on the maximum non-zero eigenvalue of A, which can be made more negative, e.g., by choosing a more negative a_1 in (33). The control input norm obtained for each agent is shown in the center of Fig. 2. At the beginning of each task, the error ε is at its maximum, and the control input increases. Around iteration 300, once the distances between agents are close to the desired ones, the affine control compensates for the distance-based terms to obtain the 15-*enclosing* formation, resulting in low-value actions. The right side of Fig. 2 shows the distance $\|{}^i q_\mu\|$ between the agents and their respective centroids, as well as the radius ρ to which they should converge in each task. Initially, only yellow agents are near their

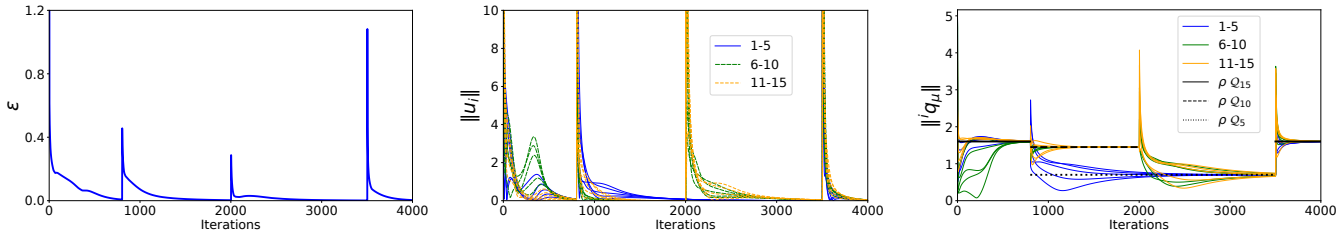

Fig. 2. Multi-target enclosing using (20). Left: Distance error ε. Center: Control input norm computed for each agent. Right: Distance between agents and their respective targets' centroid.

desired positions, while the affine control compensates the distance-based terms to reorganize blue and green agents. The term depending on ${}^i q_\mu$ is radial. Thus, the affine control needs to push the blue and green agents toward the other side of the centroid. Once these agents have passed the centroid, convergence to the desired distance becomes faster. This is the case of green agents in task 1.

It should be noted that our method does not require a global reference as in Zhang et al. (2015) or Aranda et al. (2021), and can maintain static formations without the need for orbital trajectories as in Liu et al. (2023). While existing approaches focus on stabilizing rigid patterns, as in Hara et al. (2008), or on scaling and rotating predefined shapes, as in Aranda et al. (2021), the control law (12) allows for a better fit to the geometry of the target set through affine transformations of regular polygons, e.g., ellipses, which is left as future work. Finally, the method relies on a control weights design method compatible with topologically reconfiguring the multi-agent team in a distributed manner. This could allow the team not only to obtain a single formation but also to dynamically split into multiple independent sub-formations, recalculating control weights in real time.

6. CONCLUSIONS AND FUTURE WORK

This paper proposed a distributed control method in 2D for cooperative multi-target enclosing. First, to organize agents around targets during the enclosing task, a combination of an affine formation control law with additional distance-based terms was proposed. Second, a novel weight design was presented for affine formation control of regular polygons. The distributed nature of the design allows the team of agents to locally compute control weights, a feature that can be used to reorganize into sub-formations and merge back together. We provide stability analysis of the proposed weight design, stability conditions for the enclosing law, and a simulation demonstrating the usefulness of the method when the distance between target clusters varies significantly, and it is necessary to split or merge the team. Future work involves reducing assumptions in the split and merge task and studying scalability on larger networks and robustness to noise and errors.

REFERENCES

Aranda, M., Mezouar, Y., Lopez-Nicolas, G., and Sagüés, C. (2021). Enclosing a moving target with an optimally rotated and scaled multiagent pattern. *Int. J. Control*, 94(3), 601–611.

Falconi, R., Sabattini, L., Secchi, C., Fantuzzi, C., and Melchiorri, C. (2011). A graph–based collision–free distributed formation control strategy. *IFAC Proceedings Volumes*, 44(1), 6011–6016.

Fathian, K., Rachinskii, D.I., Summers, T.H., Spong, M.W., and Gans, N.R. (2017). Distributed formation control under arbitrarily changing topology. In *Proc. Am. Control Conf*, 271–278.

Hara, S., Kim, T.H., and Hori, Y. (2008). Distributed formation control for target-enclosing operations based on a cyclic pursuit strategy. *IFAC Proceedings Volumes*, 41(2), 6602–6607.

Horn, R.A. and Johnson, C.R. (2012). *Matrix analysis*. Cambridge university press.

Khalil, H.K. and Grizzle, J.W. (2002). *Nonlinear systems*, volume 3. Prentice hall Upper Saddle River, NJ.

Lin, Z., Wang, L., Chen, Z., Fu, M., and Han, Z. (2016). Necessary and sufficient graphical conditions for affine formation control. *IEEE Trans. Autom. Control*, 61(10), 2877–2891.

Lin, Z., Wang, L., Han, Z., and Fu, M. (2014). Distributed formation control of multi-agent systems using complex Laplacian. *IEEE Trans. Autom. Control*, 59(7), 1765–1777.

Lin, Z., Wang, L., Han, Z., and Fu, M. (2015). A graph Laplacian approach to coordinate-free formation stabilization for directed networks. *IEEE Trans. Autom. Control*, 61(5), 1269–1280.

Liu, X., Liu, K., Hu, T., and Zhang, Q. (2023). Formation control for moving target enclosing via relative localization. In *Proc. IEEE Conf. Decis. Control*, 1400–1405.

López-Nicolás, G., Aranda, M., and Mezouar, Y. (2020). Adaptive multirobot formation planning to enclose and track a target with motion and visibility constraints. *IEEE Trans. Robot.*, 36(1), 142–156.

Wang, L., Han, Z., and Lin, Z. (2012). Formation control of directed multi-agent networks based on complex Laplacian. In *Proc. IEEE Conf. Decis. Control*, 5292–5297.

Wang, L., Han, Z., and Lin, Z. (2013). Realizability of similar formation and local control of directed multi-agent networks in discrete-time. In *Proc. IEEE Conf. Decis. Control*, 6037–6042.

Zhang, W., Liu, J., and Zeng, D. (2015). Multiple dynamic targets encirclement control of multiagent systems. *Mathematical Problems in Engineering*, 2015(1), 467060.

Zhao, S. (2018). Affine formation maneuver control of multiagent systems. *IEEE Trans. Autom. Control*, 63(12), 4140–4155.

Zhao, S., Dimarogonas, D.V., Sun, Z., and Bauso, D. (2018). A general approach to coordination control of mobile agents with motion constraints. *IEEE Trans. Autom. Control*, 63(5), 1509–1516.